



**HAL**  
open science

# A bisector line field approach to interpolation of orientation fields

Nicolas Boizot, Ludovic Sacchelli

► **To cite this version:**

Nicolas Boizot, Ludovic Sacchelli. A bisector line field approach to interpolation of orientation fields. 2019. hal-02193102v2

**HAL Id: hal-02193102**

**<https://univ-tln.hal.science/hal-02193102v2>**

Preprint submitted on 28 Aug 2019 (v2), last revised 18 Sep 2020 (v4)

**HAL** is a multi-disciplinary open access archive for the deposit and dissemination of scientific research documents, whether they are published or not. The documents may come from teaching and research institutions in France or abroad, or from public or private research centers.

L'archive ouverte pluridisciplinaire **HAL**, est destinée au dépôt et à la diffusion de documents scientifiques de niveau recherche, publiés ou non, émanant des établissements d'enseignement et de recherche français ou étrangers, des laboratoires publics ou privés.

# A bisector line field approach to interpolation of orientation fields

Nicolas Boizot\* and Ludovic Sacchelli\*

\* Laboratoire d'Informatique et des Systèmes, Université de Toulon, Aix Marseille Univ, CNRS UMR 7020, LIS, Marseille, France

boizot@univ-tln.fr; sacchelli@univ-tln.fr;

This research has been partially supported by the ANR SRGI (reference ANR-15-CE40-0018).

## Abstract

We propose an approach to the problem of global reconstruction of an orientation field. The method is based on a geometric model called *bisector line fields*, which maps a pair of vector fields to an orientation field, effectively generalizing the notion of doubling phase vector fields. Endowed with a well chosen energy minimization problem, we provide a polynomial interpolation of a target orientation field while bypassing the doubling phase step. The procedure is then illustrated with examples from fingerprint analysis.

**keywords:** Orientation fields; bisector line fields; polynomial interpolation; fingerprint analysis; singularities

## 1 Introduction

The present article deals with the question of global reconstruction of orientation fields on the basis of a discrete dataset. The study of these mathematical objects is motivated by the fact that they provide a very efficient model to describe the texture patterns observed in nature such as fingerprints [19, 21, 28], liquid crystals arrangements in their nematic phase [7, 10, 11] or the pinwheel structure of the visual cortex V1 of mammals [3, 4, 8, 16, 22]. For instance, in the field of fingerprints reconstruction and authentication, the estimation of ridge topologies can be a necessary step before the use of high-level classification algorithms [18, 21, 27, 28]. One can identify two kind of approaches. On the first hand, large discrete datasets can be constructed by means of a rough method such as the computation of the gradients of the fingerprint image gray intensity changes [2, 19]. However, such a strategy is prone to introduce significant noise into the data [28]. On the other hand, smaller but more reliable datasets can be obtained by using techniques focusing on the detection of stable and highly distinctive fingerprints features, such as minutiae [18, 20]. In this case, the difficulty lies in the fact that the global reconstruction of the orientation field has to be performed on the basis of scarcer information.

From the modeling point of view, an orientation field is a mapping from  $\mathbb{R}^2$  to the orientation set — that is, the interval  $[0, \pi]$  where  $\pi$  is equivalent to 0— which complicates the parametrization task. Indeed, consider the case of vector fields which are mappings from  $\mathbb{R}^2$  to  $\mathbb{R}^2$ . For a sufficiently regular vector field, singularities are identified by a rather simple criteria that can be computationally handled —*i.e.* points where the vector field vanishes. Meanwhile, singularities of orientation fields correspond to discontinuities which, for the more classic ones, translates into points where all orientations accumulate. As a consequence, in order to be able to efficiently handle orientation fields, one needs to propose a model that re-introduces some continuity property. One of the most popular solutions to this problem is the so-called *doubling phase step* [19, 20, 28] which consists in constructing a vector field by doubling the orientation field angle and taking the *cosine* and *sine* as components. This procedure transforms a mapping from  $\mathbb{R}^2$  to the orientation set into a mapping from  $\mathbb{R}^2$  to  $[-1, 1]^2$ , which resolves the orientation set's cyclicity. However, the discontinuity issue remains.

Starting from this basis, several models have been proposed in the literature, in order to reconstruct the doubling phase vector field and consequently, the orientation field [6, 9, 13, 17, 23, 24, 26, 29]. In particular,

in the seminal paper [28], the authors propose a method based on 2D Fourier Expansions to interpolate the doubling phase field, which helps address the discontinuity of the target without prior information. However, one can remark the two following points: first, this approach does not fully resolves the discontinuity issues, and second, the targeted field is not the true orientation field.

The present paper proposes to address the problem of global reconstruction of orientation fields by means of bisector line fields. This model, discussed in [5] in the framework of differential geometry, appears as a natural extension of the classical notion of doubling phase.

The *bisector line field* is an orientation field constructed from two vector fields according to the following procedure. At each point in  $\mathbb{R}^2$ , the two vector fields define two directions (in  $[0, 2\pi]$ ). The mean value of these two directions, taken modulo  $\pi$ , belongs to the orientation set and corresponds to the orientation of the line bisecting the angle between the two vector fields. This concept displays many properties that makes it an adequate tool for the global reconstruction task in the sense that, for sufficiently regular generating vector fields, the behavior of the bisector line field is very tractable. For instance, in the practical cases considered in this paper, singularities of bisector line fields happen whenever one of the two generating vector fields vanishes. As a consequence, this model organically solves the discontinuity issue discussed earlier.

The second contribution of this article is to propose an energy function that measures the error between two orientation fields directly in the orientation set. In other words, the doubling phase step is discarded. Moreover, when this energy is associated with the bisector line field model, the resulting optimization problem is particularly suited to the gradient method since the complexity of the gradient only depends on the underlying vector field structure. Therefore, although polynomial interpolation is performed in the present paper, the proposed approach might also be used with the technique presented in [28].

The rest of the article is organised as follows. Section 2 is dedicated to the definition of the bisector line field model. Important properties that justifies the approach are also exposed. Then, the interpolation method is presented in Section 3. Finally, results are displayed and discussed in Section 4.

## 2 Bisector line fields

Similarly to vector fields, orientation fields admit an intrinsic definition from the differential topology point of view, see [5] for a thorough discussion. However, such a definition lacks efficiency if one hopes to work with orientation fields and apply techniques from differential calculus. The introduction of bisector line fields is meant to bridge this gap. In the following, we only present the main notions of this model alongside with some properties relevant to the present study.

### 2.1 Notations

We use the following classical shorthands:

- $\mathbb{S}^{n-1} = \{x \in \mathbb{R}^n \mid \sum_{k=1}^n x_k^2 = 1\}$ . In particular  $\mathbb{S}^1$  is interpreted as  $[0, 2\pi]/\sim$ , the interval  $[0, 2\pi]$  where 0 is identified with  $2\pi$ ;
- $\mathbb{P}^1 = [0, \pi]/\sim$ , the interval  $[0, \pi]$  where 0 is identified with  $\pi$ .

### 2.2 Definitions and basic properties

The definitions of the several objects we manipulate are given below in a form suited to the paper's framework.

**Definition 1.** *Let  $\mathcal{D}$  denote a subset of  $\mathbb{R}^2$ .*

- *A vector field is a map  $\mathbf{X} : \mathcal{D} \rightarrow \mathbb{R}^2$ . We denote its set of zeros by  $\mathcal{Z}_{\mathbf{X}}$ .*
- *An orientation field is a map  $\mathbf{L} : \mathcal{D} \rightarrow \mathbb{P}^1$ .*
- *Let  $\mathbf{X}$  and  $\mathbf{Y}$  be two vector fields on  $\mathcal{D}$ . The bisector line field of  $(\mathbf{X}, \mathbf{Y})$  is the orientation field*

$$B(\mathbf{X}, \mathbf{Y}) : \mathcal{D} \setminus (\mathcal{Z}_{\mathbf{X}} \cup \mathcal{Z}_{\mathbf{Y}}) \rightarrow \mathbb{P}^1$$

*such that at any point  $p \in \mathcal{D}$ ,  $B(\mathbf{X}, \mathbf{Y})(p)$  is the orientation of the line bisecting the oriented pair of vectors  $(\mathbf{X}(p), \mathbf{Y}(p))$ .*

**Remark 1.** In practice, this definition implies the following. Let  $p \in \mathcal{D} \setminus (\mathcal{Z}_{\mathbf{X}} \cup \mathcal{Z}_{\mathbf{Y}})$ , there exist unique  $\theta_{\mathbf{X}}(p)$  and  $\theta_{\mathbf{Y}}(p)$  in  $\mathbb{S}^1$  such that

$$\mathbf{X}(p) = \|\mathbf{X}(p)\| \begin{pmatrix} \cos \theta_{\mathbf{X}}(p) \\ \sin \theta_{\mathbf{X}}(p) \end{pmatrix}$$

and

$$\mathbf{Y}(p) = \|\mathbf{Y}(p)\| \begin{pmatrix} \cos \theta_{\mathbf{Y}}(p) \\ \sin \theta_{\mathbf{Y}}(p) \end{pmatrix}.$$

Then, as illustrated in Figure 1,

$$\mathbf{B}(\mathbf{X}, \mathbf{Y})(p) = \frac{1}{2} (\theta_{\mathbf{X}}(p) + \theta_{\mathbf{Y}}(p)) \pmod{\pi}.$$

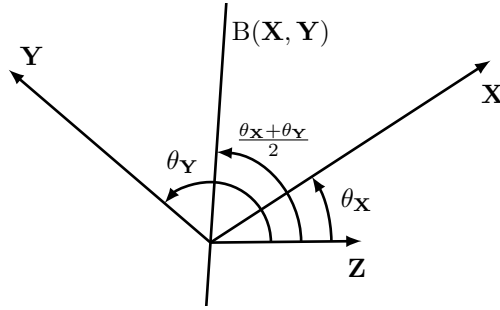


Figure 1: Representation of the bisection operation on an oriented pair of vectors, where  $\mathbf{Z} = (1, 0)'$  marks the reference vector to measure angles.

**Remark 2.** As described in the introduction, the concept of orientation field arises in different fields of applications. However, as it is a rather uncommon notion, terminology can vary between fields of study. In the context of differential geometry, the term line field is sometimes preferred, following Hopf's terminology "fields of line elements" [5, 15]. In the present article, we choose the terminology that is more popular in the fingerprint analysis community.

In our application case, singularities of orientation fields should be understood as unresolvable discontinuities of the map  $\mathbf{L} : \mathbb{R}^2 \rightarrow \mathbb{P}^1$ . To this extent, we refer in the following to continuous orientation fields  $\mathbf{L} : \mathcal{D} \rightarrow \mathbb{P}^1$ , where  $\mathcal{D}$  is the continuity domain of  $\mathbf{L}$ , and singularities of  $\mathbf{L}$  are located in  $\bar{\mathcal{D}} \setminus \mathcal{D}$ , the border of  $\mathcal{D}$ , where  $\bar{\mathcal{D}}$  denotes the topological closure of  $\mathcal{D}$ .

**Definition 2.** A continuous line field  $\mathbf{L} : \mathcal{D} \rightarrow \mathbb{P}^1$  is said to be singular at a point  $p \in \bar{\mathcal{D}} \setminus \mathcal{D}$  if it cannot be uniquely continuously extended at  $p$ .

In the following, we focus on isolated singularities, which are sufficient to our framework. In particular, we can introduce the topological index, which is a useful tool for the study of such singularities of line fields.

Let  $\mathbf{L} : \mathcal{D} \rightarrow \mathbb{P}^1$  be a continuous orientation field and let  $p$  be an isolated singularity of  $\mathbf{L}$  such that  $p$  belongs to the interior of  $\mathcal{D}$  (for instance there exists an open subset  $V$  of  $\mathbb{R}^2$  such that  $V = \{p\} \cup (V \cap \mathcal{D})$ ). Then the index of  $V$  at  $p$ , denoted  $\text{ind}_p(\mathbf{L})$ , is a half integer quantifying the winding of  $\mathbf{L}$  around  $p$  (for a precise construction of this object see, for instance, [5, Section 3.2]).

In the context of the study of orientation fields singularities, the following properties of bisector line fields arise.

**Proposition 1.** If  $\mathbf{X}$  and  $\mathbf{Y}$  are continuous vector fields over  $\mathbb{R}^2$  then  $\mathbf{B}(\mathbf{X}, \mathbf{Y})$  is continuous on  $\mathcal{D} = \mathbb{R}^2 \setminus (\mathcal{Z}_{\mathbf{X}} \cup \mathcal{Z}_{\mathbf{Y}})$ .

On the other hand, let  $\mathbf{L} : \mathcal{D} \rightarrow \mathbb{P}^1$  be a  $C^k$  orientation field, for some  $k \in \mathbb{N} \cup \{\infty\}$ . Then there exist two  $C^k$  vector fields  $\mathbf{X}, \mathbf{Y}$  over  $\mathbb{R}^2$  such that  $\mathbf{L} = \mathbf{B}(\mathbf{X}, \mathbf{Y})$ .

**Proposition 2.** *Let  $(\mathbf{X}, \mathbf{Y})$  be a pair of continuous vector fields over  $\mathbb{R}^2$ . Given an isolated point  $p$  of  $\mathcal{Z}_{\mathbf{X}} \cup \mathcal{Z}_{\mathbf{Y}}$ , we have*

$$\text{ind}_p(\mathbf{B}(\mathbf{X}, \mathbf{Y})) = \frac{1}{2}(\text{ind}_p(\mathbf{X}) + \text{ind}_p(\mathbf{Y})).$$

**Remark 3.** *An immediate consequence of this model is that singularities, initially characterized by an analytical property, now coincide with the zero sets of regular functions. In particular, isolated singularities of the bisector line field corresponds to isolated singularities of either one of the two generating vector fields.*

### 2.3 Generic properties of bisector line fields

Following Thom [25], it is understood, philosophically speaking, that “typical” behaviors of mathematical objects should be the only ones visible in nature. From the point of view of transversality theory, these typical properties are known as *generic*, in the sense that a property is generic on a topological set if it is satisfied on a residual subset. A residual subset is understood to be a large dense set in the following sense: it is a countable intersection of open and dense subsets.

For instance, the classical application case of this theory is geared towards regular maps, endowed with the  $C^k$  Whitney topology, for some  $k \in \mathbb{N}$  (see, e.g. [1, 14]).

When generic features of vector fields are considered, more can be said [5]. Example of such features are isolation of singularities of vector fields or the fact that indices of such singularities must be  $\pm 1$ .

Let  $\mathbf{X}$  and  $\mathbf{Y}$  be two smooth vector fields. Generically with respect to the  $C^2$  Whitney topology,  $\mathcal{Z}_{\mathbf{X}}$  and  $\mathcal{Z}_{\mathbf{Y}}$  are discrete collections of points that do not accumulate. Thus, singularities of  $\mathbf{X}$  and  $\mathbf{Y}$  are isolated, and moreover have  $\pm 1$  index. Furthermore, when considering  $(\mathbf{X}, \mathbf{Y})$  as a pair, we get  $\mathcal{Z}_{\mathbf{X}} \cap \mathcal{Z}_{\mathbf{Y}} = \emptyset$ .

As a consequence of these facts and Proposition 1, we get the following property for generic smooth bisector line fields, as illustrated in Figure 2.

**Proposition 3.** *Let  $(\mathbf{X}, \mathbf{Y})$  be a generic pair of vector fields. Singularities of  $\mathbf{B}(\mathbf{X}, \mathbf{Y})$  are isolated and have index  $\pm 1/2$ .*

## 3 Interpolation as an energy minimization problem

### 3.1 Discrete energy

In this section, we introduce a generalization of the least squares energy to the specific case of maps valued in  $\mathbb{P}^1$ .

Let  $d : [0, \pi] \times [0, \pi] \rightarrow [-\pi/2, \pi/2]$  be piecewise defined by

$$d(\theta_1, \theta_2) = \begin{cases} \theta_1 - \theta_2 & \text{if } |\theta_1 - \theta_2| \leq \frac{\pi}{2}, \\ \theta_1 - \theta_2 - \pi & \text{if } \theta_1 - \theta_2 > \frac{\pi}{2}, \\ \theta_1 - \theta_2 + \pi & \text{if } \theta_1 - \theta_2 < -\frac{\pi}{2}. \end{cases} \quad (1)$$

Let  $\mathcal{I}$  be a finite set and let  $(x_i, y_i)_{i \in \mathcal{I}}$  be a collection of points in  $\mathbb{R}^2$ . For  $\mathbf{M}, \mathbf{L} : \mathcal{D} \subset \mathbb{R}^2 \rightarrow \mathbb{P}^1$ , such that  $(x_i, y_i)_{i \in \mathcal{I}} \subset \mathcal{D}$ , we set the least-squares energy functional to be

$$\mathbf{J}(\mathbf{M}, \mathbf{L}) = \sum_{i \in \mathcal{I}} d(\mathbf{M}(x_i, y_i), \mathbf{L}(x_i, y_i))^2.$$

**Remark 4.** *1. The introduction of  $d$  is motivated by the following observation. Consider the energy given by  $d^2$  on the torus  $\mathbb{P}^1 \times \mathbb{P}^1$ . The gradient of  $d^2$  is*

$$\nabla d^2(\theta_1, \theta_2) = 2d(\theta_1, \theta_2)(\partial_{\theta_1} - \partial_{\theta_2})$$

*As a consequence, one can check that the gradient flow of  $d^2$  is actually parallel to the geodesic flow on the flat torus starting from the affine sets  $\{\theta_1 - \theta_2 = \pm\pi/2\}$  to the diagonal  $\{\theta_1 = \theta_2\}$  as it is illustrated in Figure 3.*

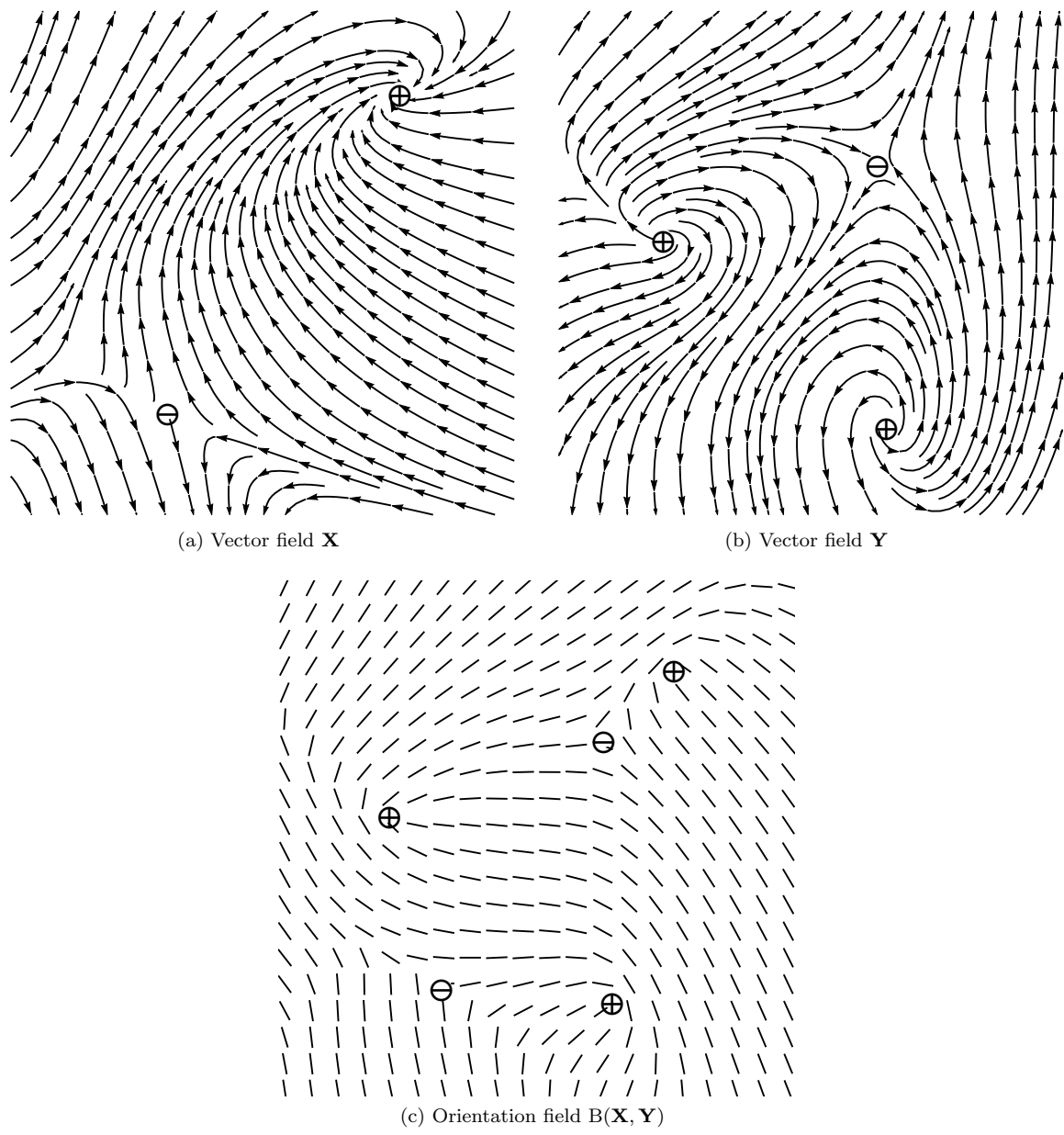


Figure 2: Example of the bisection of two vector fields. Singularities of positive index have been marked with a  $\oplus$  symbol, while singularities of negative index have been marked with a  $\ominus$  symbol.

2. The two connected components of  $\mathbb{P}^1 \times \mathbb{P}^1 \setminus \{\theta_1 = \theta_2 \pmod{\pi/2}\}$  are geodesically convex once  $\mathbb{P}^1 \times \mathbb{P}^1$  has been endowed with the flat torus Riemannian metric. Furthermore, the maps  $d_{|C}$  and  $d_{|C}^2$  are then geodesically convex and strictly geodesically convex respectively.
3. Notice that  $J^{1/2}$  is a pseudo-metric (it is symmetric and satisfies the triangular inequality) on the space of  $\mathbb{P}^1$ -valued maps over a domain containing  $(x_i, y_i)_{i \in \mathcal{I}}$ .  
Indeed  $|d|$  is a distance over  $\mathbb{P}^1$  and we de facto have the classical product metric over  $(\mathbb{P}^1)^m$  given by

$$d_m((\theta_1, \dots, \theta_m), (\theta'_1, \dots, \theta'_m)) = \left( \sum_{i=1}^m d(\theta_i, \theta'_i)^2 \right)^{1/2}$$

Then with  $m = |\mathcal{I}|$ ,

$$(\theta_1, \dots, \theta_m) = (\mathbf{M}(x_1, y_1), \dots, \mathbf{M}(x_m, y_m))$$

and

$$(\theta'_1, \dots, \theta'_m) = (\mathbf{L}(x_1, y_1), \dots, \mathbf{L}(x_m, y_m)),$$

one has

$$J(\mathbf{M}, \mathbf{L})^{1/2} = d_m((\theta_1, \dots, \theta_m), (\theta'_1, \dots, \theta'_m)).$$

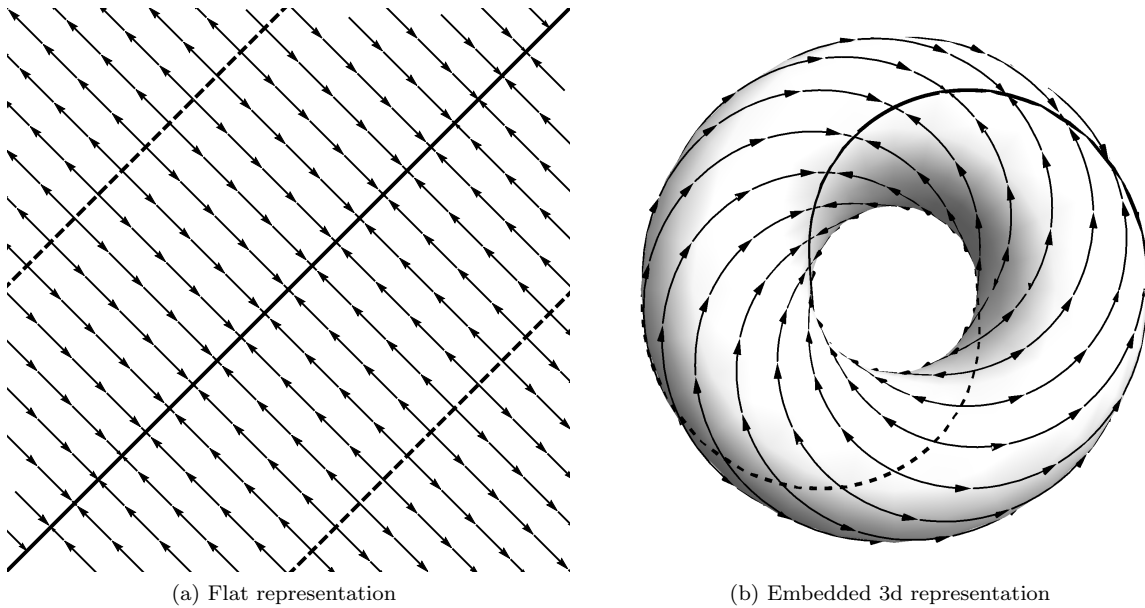


Figure 3: Representation of the gradient flow of  $d^2$  on the flat torus  $\mathbb{P}^1 \times \mathbb{P}^1$ . The set  $\{\theta_1 - \theta_2 = \pm\pi/2\}$  is denoted with a dashed line, the set  $\{\theta_1 = \theta_2\}$  is denoted with a continuous line.

### 3.2 Polynomial bisector line fields

For a given target  $\mathbf{M}$ , we minimize  $J(\mathbf{M}, \mathbf{L})$  over the set of polynomial bisector line fields of a fixed maximal degree.

Notice that for a given vector field  $\mathbf{X}$ ,  $\lambda\mathbf{X}$  yields the same direction  $\theta_{\mathbf{X}}$  for all  $\lambda > 0$ . Hence we can compactify the set of polynomial vector fields under consideration. To this extent, let us define for all  $n \in \mathbb{N}$  the set  $\mathfrak{X}^n$  of polynomial vector fields of degree  $n$  such that  $\mathbf{X} \in \mathfrak{X}^n$  if there exist  $(\alpha_{k,j})_{0 \leq j \leq k \leq n}$ ,  $(\beta_{k,j})_{0 \leq j \leq k \leq n}$  such that

$$\mathbf{X}(x, y) = \sum_{k=0}^n \sum_{j=0}^k \begin{pmatrix} \alpha_{k,j} \\ \beta_{k,j} \end{pmatrix} x^{k-j} y^j,$$

and

$$\sum_{k=0}^n \sum_{j=0}^k \alpha_{k,j}^2 + \beta_{k,j}^2 = 1.$$

In particular  $(\alpha_{k,j}, \beta_{k,j})_{0 \leq j \leq k} \in \mathbb{S}^{(n+1)(n+2)}$  and the space  $\mathfrak{X}^n$  is compact for any given  $n \in \mathbb{N}$ .  
The polynomial interpolation of the target  $\mathbf{M}$  is performed by solving, for  $m_{\mathbf{X}}, m_{\mathbf{Y}} \in \mathbb{N}$ ,

$$\min \{J(\mathbf{M}, \mathbf{B}(\mathbf{X}, \mathbf{Y})) \mid \mathbf{X} \in \mathfrak{X}^{m_{\mathbf{X}}}, \mathbf{Y} \in \mathfrak{X}^{m_{\mathbf{Y}}}\}. \quad (2)$$

Let us denote

$$1. \ n_{\mathbf{X}} = (m_{\mathbf{X}} + 1)(m_{\mathbf{X}} + 2) \text{ and } n_{\mathbf{Y}} = (m_{\mathbf{Y}} + 1)(m_{\mathbf{Y}} + 2);$$

2.  $\omega \in \mathbb{S}^{n_{\mathbf{X}}} \times \mathbb{S}^{n_{\mathbf{Y}}}$  such that

$$\omega = \left( (\alpha_{k,j}, \beta_{k,j})_{0 \leq j \leq k \leq m_{\mathbf{X}}}, (\gamma_{k,j}, \delta_{k,j})_{0 \leq j \leq k \leq m_{\mathbf{Y}}} \right);$$

$$3. \ \mathbf{X}_{\omega}(x, y) = \sum_{k=0}^{m_{\mathbf{X}}} \sum_{j=0}^k \begin{pmatrix} \alpha_{k,j} \\ \beta_{k,j} \end{pmatrix} x^{k-j} y^j$$

and

$$\mathbf{Y}_{\omega}(x, y) = \sum_{k=0}^{m_{\mathbf{Y}}} \sum_{j=0}^k \begin{pmatrix} \gamma_{k,j} \\ \delta_{k,j} \end{pmatrix} x^{k-j} y^j;$$

$$4. \ \mathbf{L}_{\omega} = \mathbf{B}(\mathbf{X}_{\omega}, \mathbf{Y}_{\omega}).$$

Problem (2) is then equivalent to solving

$$\min \{J(\mathbf{M}, \mathbf{L}_{\omega}) \mid \omega \in \mathbb{S}^{n_{\mathbf{X}}} \times \mathbb{S}^{n_{\mathbf{Y}}}\}. \quad (3)$$

### 3.3 Gradient descent approach

The function  $d$ , given in Equation (1), together with Problem (3) have been designed to allow the use of gradient based optimisation algorithms. Indeed, since

$$\mathbf{L}_{\omega}(x, y) = \frac{1}{2} (\theta_{\mathbf{X}_{\omega}}(x, y) + \theta_{\mathbf{Y}_{\omega}}(x, y)),$$

we have on  $\mathbb{R}^2 \setminus \mathcal{Z}_{\mathbf{X}_{\omega}} \cup \mathcal{Z}_{\mathbf{Y}_{\omega}}$

$$\begin{aligned} \nabla_{\omega} \mathbf{L}_{\omega} = \frac{1}{2} \left( \frac{\mathbf{X}_{\omega,1} \nabla_{\omega} \mathbf{X}_{\omega,2} - \mathbf{X}_{\omega,2} \nabla_{\omega} \mathbf{X}_{\omega,1}}{\mathbf{X}_{\omega,1}^2 + \mathbf{X}_{\omega,2}^2} \right. \\ \left. + \frac{\mathbf{Y}_{\omega,1} \nabla_{\omega} \mathbf{Y}_{\omega,2} - \mathbf{Y}_{\omega,2} \nabla_{\omega} \mathbf{Y}_{\omega,1}}{\mathbf{Y}_{\omega,1}^2 + \mathbf{Y}_{\omega,2}^2} \right), \end{aligned} \quad (4)$$

where  $(\cdot)_{\omega,i}$  denotes the  $i^{\text{th}}$  component of  $(\cdot)_{\omega}$ .

As a consequence, we can immediately compute by the chain rule

$$\nabla_{\omega} J(\mathbf{M}, \mathbf{L}_{\omega}) = -2 \sum_{i \in \mathcal{I}} d(\mathbf{M}(x_i, y_i), \mathbf{L}_{\omega}(x_i, y_i)) \nabla_{\omega} \mathbf{L}_{\omega}(x_i, y_i).$$

For  $\rho > 0$ , it should be noted that in general:

$$\omega + \rho \nabla_{\omega} J(\mathbf{M}, \mathbf{L}_{\omega}) \notin \mathbb{S}^{n_{\mathbf{X}}} \times \mathbb{S}^{n_{\mathbf{Y}}}.$$

However, we solve this issue with the projection

$$p: \mathbb{R}^{n_{\mathbf{X}}} \times \mathbb{R}^{n_{\mathbf{Y}}} \longrightarrow \mathbb{S}^{n_{\mathbf{X}}} \times \mathbb{S}^{n_{\mathbf{Y}}}$$

$$(\omega_1, \omega_2) \longmapsto \left( \frac{\omega_1}{\|\omega_1\|}, \frac{\omega_2}{\|\omega_2\|} \right).$$

Thus in the gradient descent scheme, we iterate the recursive transform

$$\omega_{k+1} \leftarrow p(\omega_k + \rho \nabla_{\omega} J(\mathbf{M}, \mathbf{L}_{\omega_k})).$$

## 4 Examples and discussion

### 4.1 Experimental setting

In order to test the paper’s approach, simulations have been performed through an implementation of a constant step-size gradient descent method in Matlab. In line with the main application of this theory—fingerprint analysis—we tested the method on elements of the FVConGoing Initiative data set [12].

More precisely, a target has been obtained with the classical elementary method of lifting the orientations of the finger ridges from the gradient of a grey-scale image of a fingerprint [19, 21]. In order to discard parts of the image that don’t correspond to the fingerprint, we neglected orientations where the gradient’s norm was too low. As a consequence, a few data corresponding to the actual fingerprint might be missing without significant effect on the result.

In the following we present three examples. The first two have been obtained with a dataset of orientations of large size but low quality. One has been performed on a classical loop fingerprint, the other on a classical whorl fingerprint. On the other hand, the third one has been obtained with a scarcer dataset of high fidelity, similar to the minutiae based methods found in [13, 23].

### 4.2 Results

The result of the interpolation experiments with large datasets are presented as follows (see Figure 4 and Figure 5). The first image is the input of the algorithm, a grey-scale image of a fingerprint. The second is a representation of the reconstructed orientation field, as a field of lines, that has been superimposed on the input.

The third and fourth images correspond to a representation of the phases of the two orientation fields, that is, grey-scale images where angles from 0 to  $\pi$  are mapped to a light intensity (near 0, dark, near  $\pi$ , bright). Image (c) is then a representation of the matrix of targeted orientations  $\bar{\mathbf{M}} = (\mathbf{M}(x_i, y_j))_{i,j}$ , while image (d) is the matrix  $\bar{\mathbf{L}} = (\mathbf{L}(x_i, y_j))_{i,j}$  of the interpolated field. Notice that the hard lines separating black and white correspond to the location of transitions from 0 to  $\pi$  in the orientation. Likewise, singularities are points where all grey levels accumulate (similar to the pinwheel singularities observed in the visual cortex [22]).

In the case of a scarce dataset, the input is a small collection of triplets  $(x, y, \theta) \in \mathbb{R}^2 \times \mathbb{P}^1$ , hence we use a different presentation of the results (see Figure 6). We include in second position a representation of these inputs as line elements on the plane, and remove the representation of the matrix  $\bar{\mathbf{M}}$ , which is no longer appropriate.

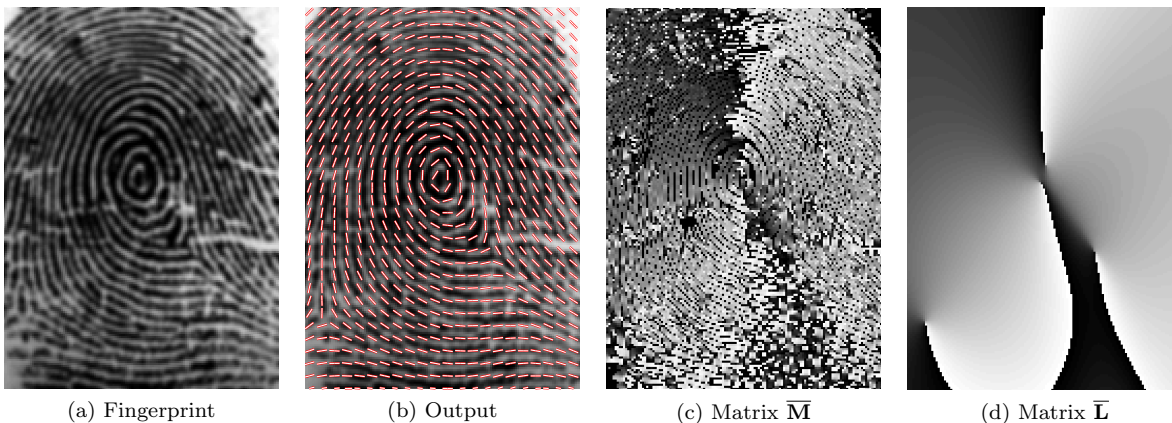


Figure 4: “Whorl” Experiment

Let us briefly comment on these results. As expected, singularities are elegantly fitted without prior knowledge of their positions. Interpolations of degree  $(3, 3)$  seem to be sufficient to obtain these results and higher order do not improve the results significantly. This is in line with other similar interpolation methods

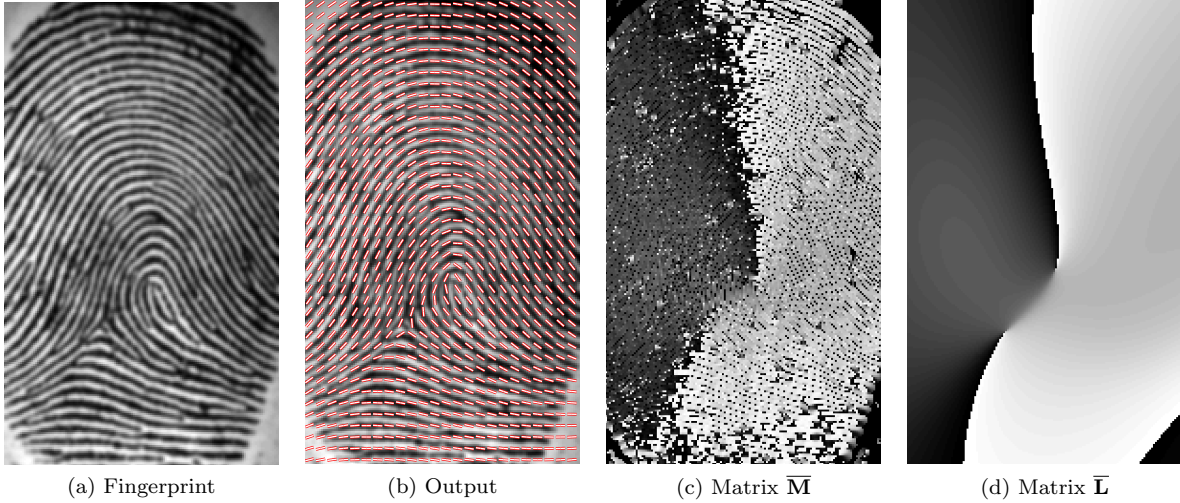


Figure 5: “Loop” Experiment

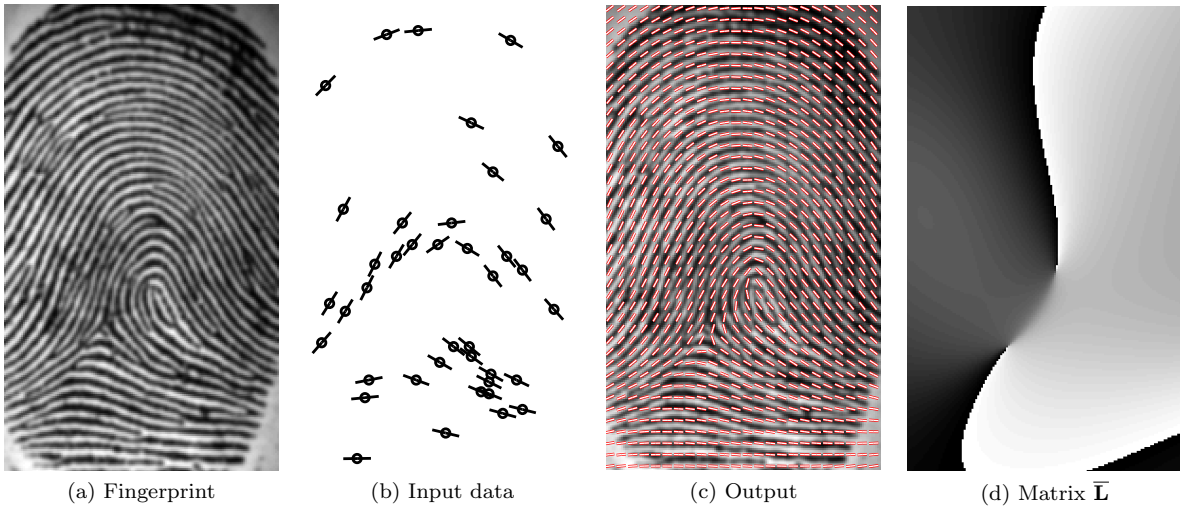


Figure 6: “Loop” Experiment with a dataset made of 40 elements

(see, for instance, the discussion on the matter in [28]). It also appears that inflexions in the orientation fields seem to be hard to fit properly (as in the lower right quarter of Figure 5). This is a weakness of the method that seems to be a general difficulty observed across the different interpolation methods we encountered in the literature. However, this does not seem to be an obstacle for the later use of finer analysis and reconstruction methods.

In the case of a sparser dataset, a moderate number of points is sufficient to recover some global information on the structure of the orientation field, such as index and curvature of certain regions. However, precise placement of the singularities is dependent on the position of elements chosen as inputs. Indeed, in the example case shown in Figure 6 a majority of data points tightly fit the singular regions which allows a good reconstruction of the underlying orientation field.

### 4.3 Discussion

As illustrated in the simulations, this choice of model is well suited to this problem. Through a rudimentary gradient based method, it is possible to recover a smooth interpolation of the targeted orientation field while discarding some of the shortcomings of prior methods. For instance the continuity issue is solved with the

introduction of the bisector model and a proper energy functional. Indeed, the doubling phase step is based on extracting a pair of discontinuous real valued functions which are, in a second step, interpolated with smooth functions. Conversely, we were able to provide a procedure that performs a smooth interpolation with the true orientation field as direct target.

Furthermore, let us mention some of the applications of the bisector line field interpolation in the context of the study of orientation fields. This generalization of the doubling phase with smooth functions allows the study of the line field with methods geared towards smooth functions. Regarding the study of singularities, it is well known that interpolation can be used to locate and describe singularities of the orientation field. In the case of bisector line field, this observation still holds true and we can illustrate it with an example. Singularities of  $B(\mathbf{X}, \mathbf{Y})$  correspond to points of  $\mathbb{R}^2$  such that either  $\mathbf{X}$  or  $\mathbf{Y}$  vanish. For instance, if  $p \in \mathbb{R}^2$  is such that  $\mathbf{X}(p) = 0$  and  $\mathbf{Y}(p) \neq 0$ , the bisector line field  $q \mapsto B(D_p \mathbf{X} \cdot q, \mathbf{Y}(p))$  acts as a linearization of  $B(\mathbf{X}, \mathbf{Y})$  at  $p$  as soon as  $D_p \mathbf{X}$  is invertible (which can be assumed as this is the generic case). As a consequence, for instance, one has in this case

$$\text{ind}_p B(\mathbf{X}, \mathbf{Y}) = \frac{1}{2} \text{sign}(\det D_p \mathbf{X}).$$

Notice that the concepts we introduced in the present paper can be adapted to fit different purposes in other scenarios. The energy we proposed is the natural choice when considering this problem and the gradient descent method is one possible direction to optimize it. Furthermore, its definition is adaptable and more can be done when information on the target is known. For instance, one can introduce weights depending on the quality of the first lift or prior knowledge of the singularity locations.

Finally, solving this optimization problem on the set of polynomial vector fields of a fixed degree is not a requirement of the method. What is actually necessary to solve the problem with this methodology is the introduction of a family of smooth functions that serves as a basis for the space of regular vector fields on a bounded domain of  $\mathbb{R}^2$ . Hence this entire method can be adapted to the classical case of trigonometric polynomials.

## 5 Conclusion

In this paper we proposed a solution to the problem of interpolation of orientation fields with smooth functions. To this end, we introduced a methodology based on the bisector line field model associated with a well suited energy functional. On the one hand, the bisector model has the double virtue of generalizing known techniques from the field of fingerprint analysis while resolving the continuity issues from the classical approach. On the second hand, the energy is coherent with unique aspects of this problem on the space of orientation fields and facilitates to use of gradient descent methods. Finally, the procedure has been applied to perform polynomial interpolation of orientation fields in the framework of fingerprint analysis.

## References

- [1] R.H. Abraham and J.W. Robbin. *Transversal Mappings and Flows*. Benjamin, 1967.
- [2] A.M. Bazen and S.H. Gerez. Systematic methods for the computation of the directional fields and singular points of fingerprints. *IEEE Transactions on Pattern Analysis and Machine Intelligence*, 24(7):905–919, 2002.
- [3] U. Boscain, R. A. Chertovskih, J. P. Gauthier, and A. O. Remizov. Hypoelliptic diffusion and human vision: A semidiscrete new twist. *SIAM Journal on Imaging Sciences*, 7(2):669–695, 2014.
- [4] U. Boscain, J. Duplaix, J-P. Gauthier, and F. Rossi. Anthropomorphic image reconstruction via hypoelliptic diffusion. *SIAM Journal on Control and Optimization*, 50(3):1309–1336, 2012.
- [5] U. Boscain, L. Sacchelli, and M. Sigalotti. Generic singularities of line fields on 2d manifolds. *Differential Geometry and its Applications*, 49:326–350, 12 2016.

- [6] R. Cappelli, D. Maio, A. Lumini, and D. Maltoni. Fingerprint image reconstruction from standard templates. *IEEE Transactions on Pattern Analysis and Machine Intelligence*, 29(9):1489–1503, 2007.
- [7] S. Chandrasekhar. *Liquid Crystals*. Cambridge University Press, 2nd edition, 1992.
- [8] G. Citti and A. Sarti. A cortical based model of perceptual completion in the roto-translation space. *Journal of Mathematical Imaging and Vision*, 24(3):307–326, 2006.
- [9] S.C. Dass. Markov random field models for directional field and singularity extraction in fingerprint images. *IEEE Transactions on Image Processing*, 13(10):1358–1367, 2004.
- [10] P.G. de Gennes and J. Prost. *The Physics of Liquid Crystals*. Number 83 in International Series of Monographs on Physics. Clarendon Press, 1995.
- [11] S. J. DeCamp, G. S. Redner, A. Baskaran, M. F. Hagan, and Z. Dogic. Orientational order of motile defects in active nematics. *Nature Materials*, 14(11):11101115, 2015.
- [12] B. Dorizzi, R. Cappelli, M. Ferrara, D. Maio, D. Maltoni, N. Houmani, S. Garcia-Salicetti, and A. Mayou. Fingerprint and on-line signature verification competitions at ICB 2009. In *Advances in Biometrics*, pages 725–732. Springer Berlin Heidelberg, 2009.
- [13] J. Feng and A. K. Jain. Fingerprint reconstruction: From minutiae to phase. *IEEE Transactions on Pattern Analysis and Machine Intelligence*, 33(2):209–223, 2011.
- [14] Morris W. Hirsch. *Differential Topology*. Springer New York, 1976.
- [15] H. Hopf. Part II, chapter 3, The Total Curvature (Curvatura Integra) of a Closed Surface with Riemannian Metric and Poincaré’s Theorem on the Singularities of Fields of Line Elements. In *Differential geometry in the large: seminar lectures New York University 1946 and Stanford University 1956*. Springer, 2003.
- [16] D. H. Hubel and T. N. Wiesel. Receptive fields, binocular interaction and functional architecture in the cats visual cortex. *The Journal of physiology*, 160(1):106–154, 1962.
- [17] J. Zhou and J. Gu. A model-based method for the computation of fingerprints’ orientation field. *IEEE Transactions on Image Processing*, 13(6):821–835, 2004.
- [18] T. Joshi, S. Dey, and D. Samanta. A two-stage algorithm for core point detection in fingerprint images. In *TENCON 2009 - 2009 IEEE Region 10 Conference*. IEEE, 2009.
- [19] M. Kass and A. Witkin. Analyzing oriented patterns. *Computer Vision, Graphics, and Image Processing*, 37(3):362 – 385, 1987.
- [20] S. Li and A. C. Kot. An improved scheme for full fingerprint reconstruction. *IEEE Transactions on Information Forensics and Security*, 7(6):1906–1912, 2012.
- [21] D. Maltoni, D. Maio, A. K. Jain, and S. Prabhakar. *Handbook of Fingerprint Recognition*. Springer Publishing Company, Incorporated, 2nd edition, 2009.
- [22] Jean Petitot. *Elements of Neurogeometry*. Springer, 2017.
- [23] A. Ross, J. Shah, and A. K. Jain. From template to image: Reconstructing fingerprints from minutiae points. *IEEE Transactions on Pattern Analysis and Machine Intelligence*, 29(4):544–560, 2007.
- [24] B. G. Sherlock, D. M. Monro, and K. Millard. Fingerprint enhancement by directional fourier filtering. *IEE Proceedings - Vision, Image and Signal Processing*, 141(2):87–94, 1994.
- [25] R. Thom. *Stabilité structurelle et morphogénèse*. W. A. Benjamin, Inc., Reading, Mass., 1972. Essai d’une théorie générale des modèles, Mathematical Physics Monograph Series.
- [26] P. R. Vizcaya and L. A. Gerhardt. A nonlinear orientation model for global description of fingerprints. *Pattern Recognition*, 29(7):1221–1231, 1996.

- [27] Y. Wang and J. Hu. Global ridge orientation modeling for partial fingerprint identification. *IEEE Transactions on Pattern Analysis and Machine Intelligence*, 33(1):72–87, 2011.
- [28] Y. Wang, J. Hu, and D. Phillips. A fingerprint orientation model based on 2d fourier expansion (FOMFE) and its application to singular-point detection and fingerprint indexing. *IEEE Transactions on Pattern Analysis and Machine Intelligence*, 29(4):573–585, April 2007.
- [29] J. Zhou and J. Gu. Modeling orientation fields of fingerprints with rational complex functions. *Pattern Recognition*, 37(2):389–391, 2004.